Hindawi Publishing Corporation
Advances in Optical Technologies
Volume 2012, Article ID 754546, 11 pages
doi:10.1155/2012/754546

Review Article

High-Quality Growth of GaInNAs for Application to Near-Infrared Laser Diodes

Masahiko Kondow and Fumitaro Ishikawa

Graduate School of Engineering, Osaka University, 2-1 Yamada-oka, Suita, Osaka 565-0871, Japan

Correspondence should be addressed to Masahiko Kondow, kondow@eei.eng.osaka-u.ac.jp

Received 27 June 2012; Accepted 4 September 2012

Academic Editor: Marija Strojnik

Copyright © 2012 M. Kondow and F. Ishikawa. This is an open access article distributed under the Creative Commons Attribution License, which permits unrestricted use, distribution, and reproduction in any medium, provided the original work is properly cited.

GaInNAs was proposed and created in 1995. It can be grown pseudomorphically on a GaAs substrate and is a light-emitting material with a bandgap energy that corresponds to near infrared. By combining GaInNAs with GaAs, an ideal band lineup for laser-diode application is achieved. This paper presents the reproducible growth of high-quality GaInNAs by molecular beam epitaxy. Examining the effect of nitrogen introduction and its correlation with impurity incorporation, we find that Al is unintentionally incorporated into the epitaxial layer even though the Al cell shutter is closed, followed by the concomitant incorporation of O and C. A gas-phase-scattering model can explain this phenomenon, suggesting that a large amount of N_2 gas causes the scattering of residual Al atoms with occasional collisions resulting in the atoms being directed toward the substrate. Hence, the reduction of the sublimated Al beam during the growth period can suppress the incorporation of unintentional impurities, resulting in a highly pure epitaxial layer.

1. Introduction to GaInNAs for Application to Near-Infrared Laser Diodes

GaInNAs was proposed and created in 1995 by Kondow et al. [1, 2]. It is is a member of the family of dilute nitrides and III-N-V alloys, such as GaNP and GaNAs, which are novel semiconductor materials developed in the 1990s. A couple of research groups reported on III-N-V alloy semiconductors before 1994 [3–6]. However, these reports have been limited to crystal growth and measurements of physical properties. Kondow et al. proposed application of dilute nitrides to optoelectronic devices [1, 2] because the exceptional physical properties of III-N-V alloy semiconductors, such as their huge degrees of bandgap bowing, facilitate devices with levels of performance greatly superior to those of current devices. The unusual physical properties are consequences of the exceptional chemical characteristics of N as compared to the other elements in groups III and V. However, these chemical characteristics lead to difficulties in the creation of alloys of N and III-V crystals, that is, in the growth of III-N-V alloys. A strongly nonequilibrium method of growth and highly reactive N precursor are essential to overcome the immiscibility of N in III-V alloys. For this reason, no one had succeeded in growing any such material before the early 1990s. Kondow et al. proposed and developed a growth method for III-N-V alloys in 1994 [7]. They adopted molecular beam epitaxy (MBE) with N supplied in the form of radicals. Their method has subsequently been widely used as a standard method for growing III-N-V alloys with excellent crystallinity. In 1996, S. Sato et al. succeeded in growing GaInNAs with excellent crystallinity by conventional organometallic vapor-phase epitaxy (OMVPE) [8], despite the failure of several groups. In general, the advantages of OMVPE are its applicability to the fabrication of complex layered structures, good reproducibility of growth from run to run, and suitability for use in mass production. The availability of both growth methods has accelerated research in III-N-V alloys and the development of devices based on these materials.

GaInNAs is a light-emitting material with a bandgap energy suitable for near-infrared laser diodes (LDs) (1.3–1.55 μm and longer wavelengths) and can be grown pseudomorphically on a GaAs substrate. Combining GaInNAs with GaAs or any other wide-gap materials that can be grown

on a GaAs substrate results in a type I band lineup for applying a material to the quantum-well active layer of an LD. A type I band lineup is essential for both electrons and holes to be confined to the quantum-well layer. This allows the fabrication of very deep quantum wells, especially in the conduction band. Deep quantum wells provide many advantages in terms of LD performance, as shown later.

In this section, we start by examining the bandgap structure of GaNAs and GaInNAs. Next, we explain the band lineup of GaNAs and GaInNAs. Then we present quantum levels in a GaInNAs/GaAs well. Finally, we discuss the advantages of GaInNAs in the application of LDs.

Figure 1 shows the experimentally obtained relationship between the N content and bandgap energy of GaNAs epilayers grown on a GaAs substrate [7]. The N content was estimated using X-ray diffraction, and the bandgap energy was measured by photoluminescence (PL). As for GaNAs with a low N content, the PL peaks of the GaNAs epilayer and the GaAs substrate overlapped when measurement was taken at room temperature. Therefore, PL was also observed at the very low temperature of 77 K. The bandgap energy decreased monotonically with increased N content. The energy difference between room temperature and 77 K measurements hardly varied, remaining at approximately 70 meV. The lines denoting room temperature and 77 K measurement thus run parallel in this figure. The slope of each line is 0.184 eV/% N. The GaNAs epilayers grown on a GaAs substrate were under tensile strain, which lowers the bandgap energy. To determine the relationship between the N content and bandgap energy of free standing, that is, stress-free, GaNAs, the bandgap energy was calibrated using the deformation potential parameters for GaAs. The results are shown as broken lines having a slope of 0.156 eV/% N in Figure 1.

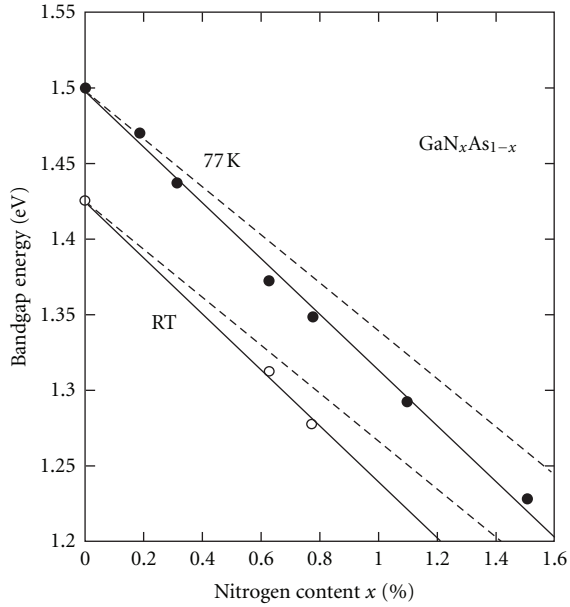

Figure 1: The relationship between N content and bandgap energy of GaNAs epilayers grown on a GaAs substrate [7]. The solid lines are experimental results. Broken lines are the result of calibration to remove the effect of strain.

Figure 2 shows the relationship between the lattice constant and bandgap energy in various III-V alloy semiconductors, including GaNAs and GaInNAs [9]. The bowing parameter of GaNAs was derived from the above experimental results for GaNAs with a small N content [7], assuming a parabolic curve [10]. With conventional alloy semiconductors, the results for which lie in the shaded area of Figure 2, the tendency is for the bandgap energy to increase with a decreasing lattice constant. On the other hand, the result for GaNAs departs from the shaded area to which conventional alloy semiconductors are restricted. Until N comes to make up half of the GaNAs, an increase in N content leads to a monotonic decrease in bandgap energy rather than an increase towards the value for cubic GaN (3.2 eV). This curious behavior is supported by both experimental results [6] and theoretical predictions [10]. The responsible factor is the large discrepancy between the electronegativity values for N and the other constituent atoms [10]. Phillips states that the electronegativity of N is 3.00, while the values for P, As, and Sb are from 1.31 to 1.64 [11]. Since one property of III-N-V alloy semiconductors is that a decrease in the lattice constant leads to a decrease in the bandgap energy, they provide operation over a dramatically broader area than conventional III-V alloy semiconductors, as shown in Figure 2. This leads to significantly greater freedom in the design of semiconductor devices, to the extent that novel devices and dramatic improvements in the performance of current devices become possible. This figure includes results for GaNAs, which might possibly have a negative bandgap energy for large N concentrations. This might mean that GaNAs can act as a metal or semiconductor, according to the N content. While such behavior is very interesting, there is no reliable experimental data on this region because of phase separation. Furthermore, there is no guarantee that bandgap theory can be expanded to cover this region. Thus, the middle range of III-N-V alloy composition remains unexplored.

Let us focus on the bandgap energy of GaInNAs. Adding In to GaAs, that is, making a GaInAs-alloy semiconductor, increases the lattice constant, while adding N to GaAs, that is, making a GaNAs-alloy semiconductor, decreases the lattice constant. GaInNAs can thus be lattice matched to GaAs by adjusting the contents of In and N. Adding In to GaAs decreases the bandgap, and in the same way, adding N to GaAs also decreases the bandgap, as shown in Figure 2. Since both GaInAs and GaNAs are direct-transition-type semiconductors, GaInNAs is also of this type. Thus, GaInNAs is a light-emitting material that has a bandgap energy suitable for near-infrared laser diodes (0.8–1.0 eV) and is suitable for formation on a GaAs substrate.

Figure 3 shows the N-content dependence of the band-discontinuity energy in the valence band (ΔE_v) for GaNAs/GaAs measured using X-ray photoelectron spectroscopy (XPS) [12]. The rather large experimental error was due to the limited energy resolution in this measurement. The center value of ΔE_v for GaNAs decreased as the N content increased. This suggests the formation of a type

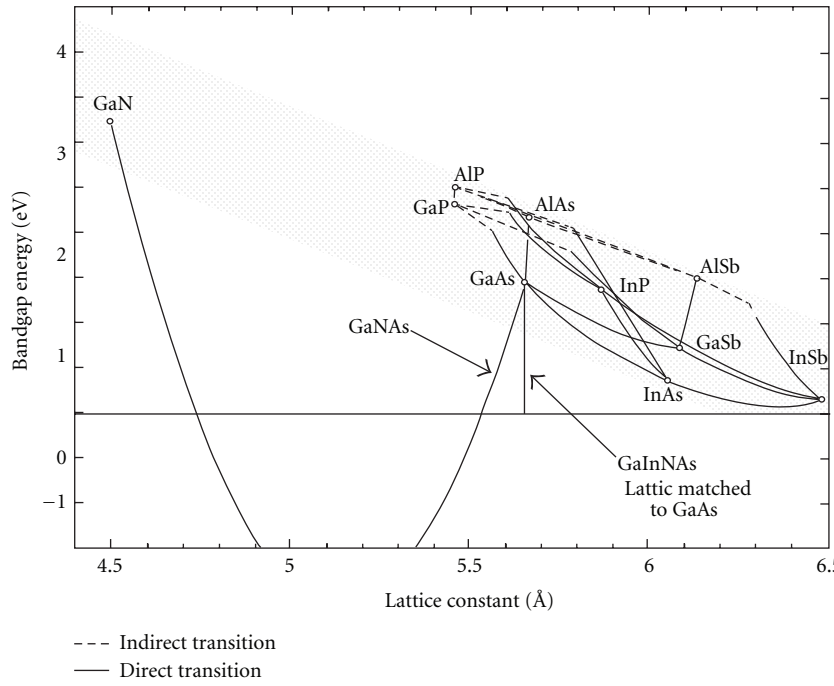

Figure 2: The relationship between lattice constant and bandgap energy in III-V alloy semiconductors [9].

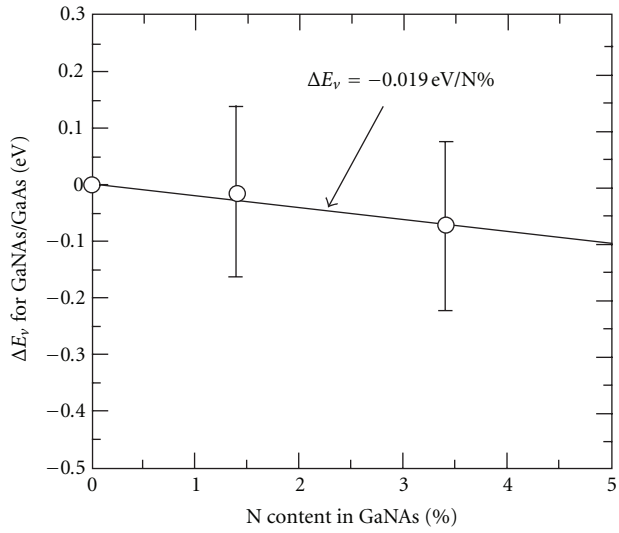

Figure 3: Dependence of ΔE_v on the content of N in GaNAs/GaAs [12].

II band lineup in GaNAs/GaAs. From the slope, ΔE_v for GaNAs/GaAs was estimated as $-(0.019 \pm 0.053)$ eV/%N (the large experimental error means that there is still a possibility that a type I band lineup will form in GaNAs/GaAs). Ding et al. reported ΔE_v of -1.84 eV in cubic-GaN/GaAs based on XPS measurement [13]. If the ΔE_v of cubic-GaN/GaAs is linearly interpolated, ΔE_v of GaNAs/GaAs can be calculated as -0.0184 eV/%N. This is in good agreement with the above measured value of -0.019 eV/%N. Thus, bandgap bowing seems to have little effect on the ΔE_v of GaNAs, and this result supports the theoretical prediction by Sakai et al. in which bowing of the valence band of GaNAs is negligible [14].

Next, the band lineup of the GaInNAs materials system is examined from the viewpoint of application to an LD because a type I band lineup is essential for both electrons and holes to be confined to the quantum-well layer in order to apply a material to the quantum-well active layer of an LD.

A schematic diagram of the bandgap for GaInAs is shown in the right half of Figure 4, and the bandgap of GaNAs is shown in the left half. The horizontal axis shows strain, which allows us to draw the diagrams for GaInAs and GaNAs in the same figure. GaAs is therefore located in the center. In Figure 4, bowing of the valence band of GaNAs is assumed to be zero on the basis of the experimental results cited previously [12]. As a result, both the conduction band and bandgap have the same bowing parameter in the GaNAs system. Thus, the bowing of the conduction band is very large. Increasing the In content in GaInAs, that is, increasing the compressive (+) strain, lowers the conduction band and raises the valence band. On the other hand, increasing the N content in GaNAs, that is, increasing the tensile (−) strain, lowers both the conduction and valence bands. Since the conduction band falls more steeply than the valence band, increasing the N content decreases the bandgap. If a small amount of N is added to GaInAs to form GaInNAs, the conduction and valence bands will be moved from A to B and from D to E (Figure 4). When the composition is such that GaInNAs is lattice-matched with GaAs, the conduction band will be at C and the valence band will be at F. Note that the valence bands of the GaInNAs and GaAs are at almost the same energy level. Therefore, by combining GaInNAs with

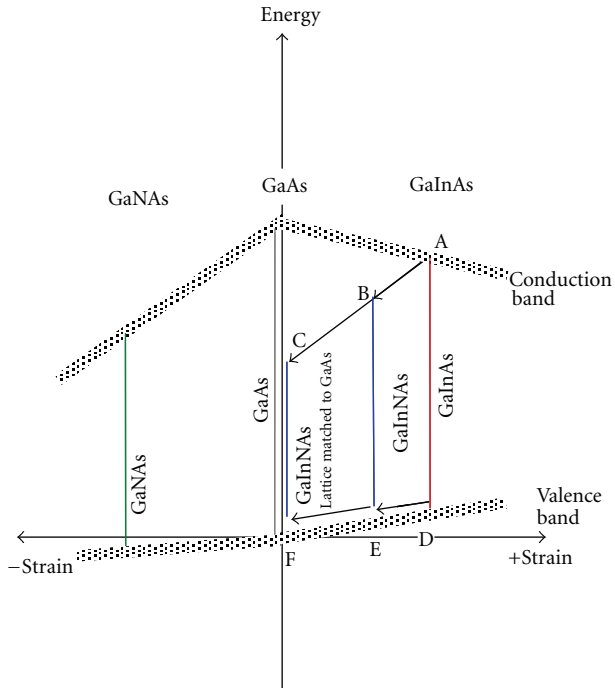

Figure 4: Schematic diagram of bandgap of GaInAs, GaNAs, and GaInNAs. For lattice matching of GaInNAs to GaAs, In concentration is required to be approximately 3 times of N concentration. For example, $Ga_{0.90}In_{0.10}N_{0.035}As_{0.965}$ is lattice-matched.

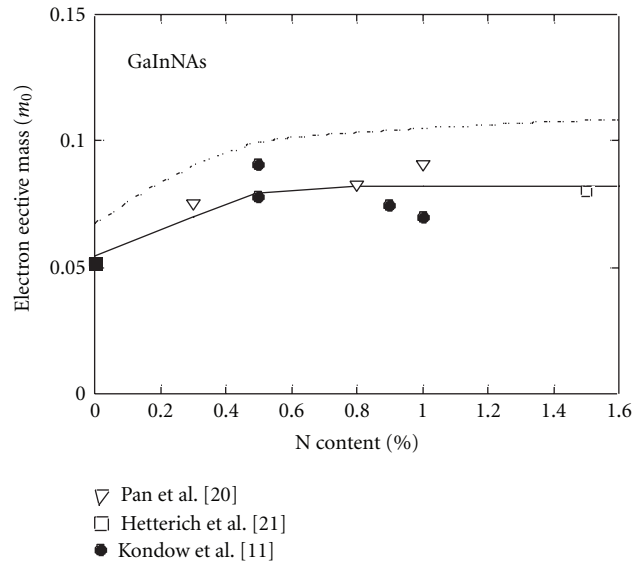

Figure 5: The effective mass of an electron in GaInNAs as a function of the content of N [15]. Broken line denotes a theory for GaNAs [16].

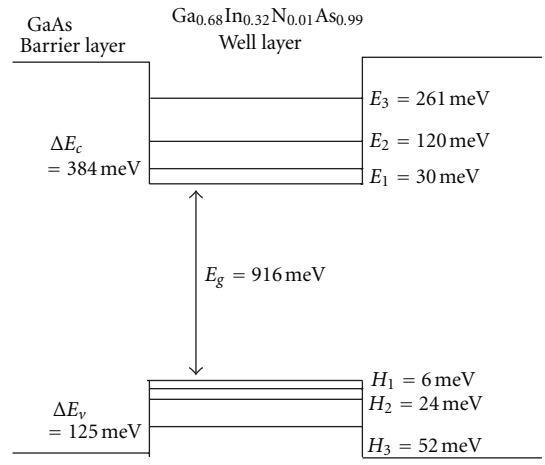

Figure 6: The quantum levels in a 10 nm thick $Ga_{0.68}In_{0.32}N_{0.01}A_{0.99}$/GaAs well with an emission wavelength of 1.31 μm.

wide-gap materials, such as AlGaAs, a type I band lineup is easily achieved. Compressively (+) strained GaInNAs can also have a type I band lineup in combination with GaAs. In general, a ΔE_v of more than 50 meV is required to confine holes to the quantum-well layer. Since the GaInAs quantum-well layer in a 0.98 μm range laser diode formed on a GaAs substrate is strained by approximately 1% and has a ΔE_v as high as 50 meV, compressively strained GaInNAs has to be strained by at least 1% to achieve good hole confinement (in this case, the GaInNAs should be grown as a strained quantum-well layer that is thinner than the critical thickness where misfit dislocations start to appear). The conduction band of GaInNAs, whether it is lattice-matched to GaAs or compressively strained, has a large discontinuity energy (ΔE_c).

Next, we discuss the quantum levels in GaInNAs/GaAs wells. Knowledge of the effective masses of individual holes and electrons is necessary if we are to determine these levels. As mentioned above, alloying Ga (In) As with N strongly affects the conduction band but has little effect on the valence band. Therefore, we may assume the effective mass of a hole in GaInNAs to be the same as that of a hole in GaInAs with the same In content. On the other hand, the effective mass of an electron in GaInNAs differs greatly from that of an electron in GaInAs. Figure 5 shows this effective mass as a function of the N content. This result was obtained by analyzing the optical transitions between the ground levels [17] and high-order quantum levels [15, 18] in GaInNAs/GaAs quantum wells. Note that the transition energies between the high-order quantum levels are sensitive to the mass value. Therefore, we can thus obtain precise values through this approach. The effective mass remains in the range $0.08 \pm 0.01\, m_0$ (where m_0 is the mass of a free electron) almost independently of the N content. This behavior is in good agreement with a theoretical prediction for GaNAs [16]. An electron has a 60% larger effective mass in $Ga_{0.7}In_{0.3}NAs$ than in $Ga_{0.7}In_{0.3}As$.

Figure 6 is a sketch of the quantum levels in a $Ga_{0.68}In_{0.32}N_{0.01}A_{0.99}$/GaAs well, a system that produces emission at 1.31 μm. The well is 10 nm thick. The strain of the well is about +2%. The energy difference between electrons at the first and second quantum levels is 90 meV. Thus, most

electrons are on the ground level. This leads to a large optical gain for the LD.

Deep quantum wells provide many advantages in terms of LD performance, including high operating speeds and excellent temperature stability of threshold current (I_{th}) and lasing wavelength. GaInNAs is also promising as a material for use in near-infrared vertical-cavity surface-emitting lasers (VCSELs), because a GaInNAs active layer can be grown on a highly reflective GaAs/AlAs distributed Bragg reflector (DBR) mirror over a GaAs substrate in a single stage of epitaxial growth [19]. GaInNAs can be grown by both OMVPE and MBE. However, LDs with a long lifetime is limited to MBE-grown devices [20, 21]. Therefore, from the viewpoint of industry use, MBE growth is important for GaInNAs. Currently MBE-grown GaInNAs VCSELs are on the market [21].

2. Unintentional Al Incorporation during GaInNAs Growth

2.1. Background. The features of GaInNAs material may come from the large electron negativity difference between III-nitride compounds and other III-V compounds. However, the large electron negativity and large atomic size differences also make obtaining a high-quality crystal difficult. Researchers worldwide have devoted much effort to improving the crystallinity of this novel material [22]. As a result, the threshold current density (J_{th}) of 1.3 μm range GaInNAs LDs has been reduced to as low as that of LDs made of conventional materials [23, 24]. However, this is still higher than that of LDs made of GaInAs, that is, the host material of GaInNAs. Therefore, the maximum performance of GaInNAs LDs has not yet been achieved. Some experimental studies have revealed that GaInNAs LDs still exhibit serious nonradiative recombination [25, 26].

Nonradiative recombination may be related to intrinsic and extrinsic defects. GaInNAs is thermodynamically metastable or unstable. Therefore, careful optimization of both growth and postannealing is necessary. Much effort by many researchers worldwide has been devoted to such optimization to reduce intrinsic defects [22]. However, the results have not been satisfactory, as mentioned above. Therefore, extrinsic defects in GaInNAs should now be studied. Aluminum was detected in OMVPE-grown GaInNAs grown over an AlGaAs layer [27–29]. According to Takeuchi et al. [27], Al generates three-dimensional growth and degrades the crystallinity of a GaInNAs active layer and LD performance.

GaInNAs can be grown by both OMVPE and MBE. However, LDs with a long lifetime are limited to MBE-grown devices [20, 21]. Therefore, from the viewpoint of industry use, MBE growth is important for GaInNAs. Kondow et al. investigated extrinsic impurities in MBE-grown GaInNAs [30]. They used 1.3 μm range GaInNAs LDs with $Al_{0.3}Ga_{0.7}As$ cladding layers as specimens. Thus, the $Ga_{0.7}In_{0.3}N_{0.01}As_{0.99}$ active layer was grown over an AlGaAs layer. The LDs were grown using a solid-source MBE system with an N plasma cell [31]. Their N_2 gas line from an N_2 cylinder to a plasma cell did not have any material containing Al. It had two inline purifiers, MILLIPORE Waferpure, which remove H_2O, O_2, CO, and CO_2 from N_2 gas. The gas line was kept in a high vacuum at around 1×10^{-8} Torr using a vent/run system when N_2 gas was not introduced. Figure 7 shows a cross section of the LDs they studied. The active layer had a single quantum well (SQW) with a thickness of 7 or 10 nm sandwiched between two 150 nm thick GaAs layers. The cladding layers were each 1.5 μm thick and had a carrier density of approximately 1×10^{18} cm^{-3}. A p-GaAs contact layer ($p = 1 \times 10^{19}$ cm^{-3}) was formed to decrease the contact resistance. The ridge mesa width was approximately 2 μm, and the cavity length was 400 μm. Facets were as cleaved. This LD structure is likely one standard for the GaInNAs LD. The typical I_{th} of GaInAs LDs grown using their MBE system is 10 mA. This value is quite reasonable as a GaInAs LD under this LD structure. On the other hand, the GaInNAs LDs Kondow et al. investigated had an I_{th} of 60–70 mA.

To examine what residual molecules exist in their MBE chamber, experiments using quadrupole-mass spectrometry (QMS) were conducted under high sensitivity when N_2 gas was not introduced into the chamber. The peaks corresponding to the residual molecules of H_2, H_2O, CO, N_2, or CO_2 were observed at 2, 18, 28, and 44 a.m.u., respectively, rather than those related to As at 37, 38 and 75 a.m.u. More specifically, the peaks at 2 and 18 a.m.u. accompanied peaks at 1 and at 16 and 17 a.m.u., respectively, because H_2, H_2O were cracked in a QMS analyzer. Hence, the candidates of the extrinsic impurities in the GaInNAs crystal are H, C, and O. Note that no signal corresponding to O_2 was detected at 32 a.m.u. Considering the lack of O_2 and the typical I_{th} value for GaInAs LDs, their MBE system was prepared well and had no problem at least in growing conventional III-V materials.

The concentrations of impurities in the GaIn(N)As active layer were measured using secondary ion mass spectrometry (SIMS). Figure 8 shows the relationship between the impurity concentrations and I_{th} of the LDs. The I_{th} does not depend on H or C concentration. Since the respective concentrations for H and C at 1×10^{17} and 1×10^{16} cm^{-3} were the detection limit in the SIMS measurement for their study, actual concentrations for H and C might be lower than these values. While we cannot determine the real relationship between I_{th} and H or C concentration, it is likely that the respective concentrations for H and C at 1×10^{17} and 1×10^{16} cm^{-3} are too low to affect I_{th}. On the other hand, I_{th} increased as the O concentration increased (concentration of O at 2×10^{16} cm^{-3} is the detection limit.). The O concentration dependence of I_{th} in the figure means that O is the main impurity that must be reduced to 2×10^{16} cm^{-3} or less.

Although the O concentrations in the GaInAs and GaInNAs active layers are the same at 4×10^{16} cm^{-3}, there is a considerable difference in I_{th} among these LDs. Therefore, some other impurity may exist in GaInNAs. When Kondow et al. considered the QMS results and the fact that the precursors used in the MBE were extremely pure, it was hard to believe that any atoms other than the precursors for the LDs could provide the unknown impurity. Thus, they checked for Al by using SIMS. They prepared samples of which the upper cladding layer was mostly etched off because it was

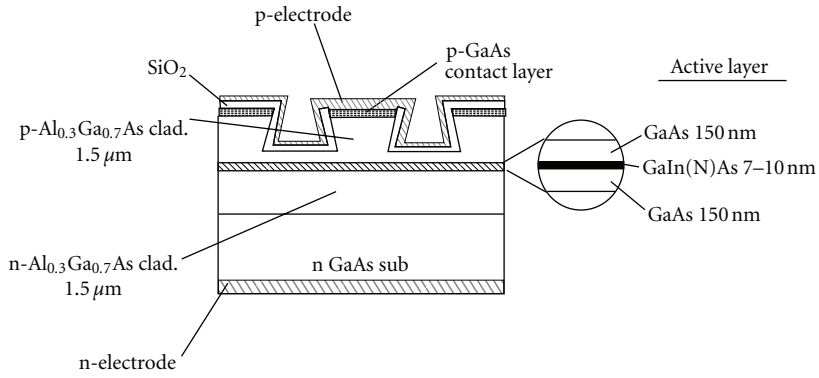

Figure 7: Cross section of the GaIn(N)As LDs used in the study [30].

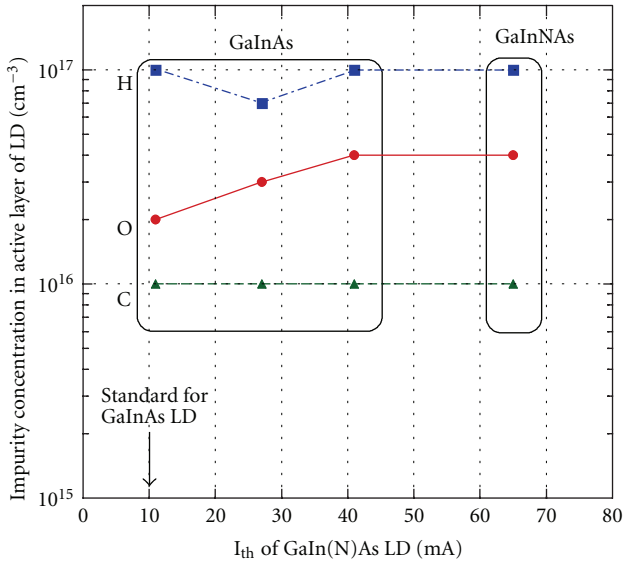

Figure 8: Relationship between the impurity concentrations and I_{th} of the GaIn(N)As LDs [30].

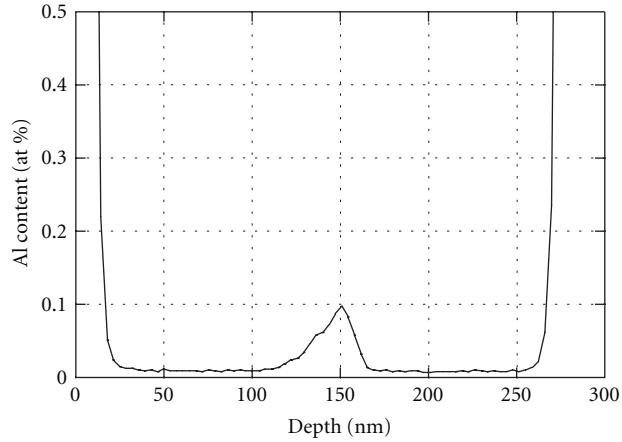

Figure 9: Al depth profile measured by SIMS [30].

difficult to detect the Al signal at the GaInNAs quantum-well position in a sample with a whole layer structure due to a relatively high etching speed. Figure 9 shows an Al depth profile. Both sides correspond to the AlGaAs cladding layers. There was a distinct Al peak at the center of the GaInNAs/GaAs active layer (i.e., the position of the GaInNAs quantum well), even though Al was never supplied during GaInNAs growth. The Al concentration was as much as 0.1%. Coincidently, this value agrees with that in OMVPE-grown GaInNAs [27]. According to Takeuchi et al. [27], Al generates three-dimensional growth and degrades the crystallinity of GaInNAs. Although the growth mechanism and the Al supply mechanism are different for OMVPE and MBE, it may be possible that GaInNAs is degraded by three-dimensional growth if 0.1% Al is incorporated. The Al incorporation in MBE may depend on the plasma condition of an N plasma cell and the inside structure of the growth chamber.

2.2. Investigation of Al Incorporation Mechanism. Ishikawa et al. investigated the origin of the unintentional incorporation of Al during plasma-assisted MBE growth [32]. They grew samples having a GaNAs/GaAs/AlAs stacked structure at 450°C. Prior to growing the structure, a 200 nm GaAs buffer layer was grown at 580°C. They grew a 1 μm thick AlAs layer on the buffer to make the growth situation similar to that of the laser structure. The growth was carried out without interruption throughout the structure. After the growth of the AlAs layer, the shutter of the Al cell was closed and the shutter of Ga cell was opened simultaneously. Then, the Al source temperature was kept at the growth temperature of 1020°C until the end of full-structure growth. The growth of GaNAs with plasma-assisted MBE requires many operations. They grew the sample shown in Figure 10 with the procedure summarized in the same figure. They considered the layer grown with bright mode N plasma with its shutter opened as the GaNAs layer. There are 16 steps, labeled (i)–(xvi). They carried out the listed operations at the beginning of every step. They maintained the growth condition for 5 min, corresponding to the growth of 83 nm for each layer. However, step (i) was maintained for 10 min, growing 166 nm to prevent Al diffusion, as reported by

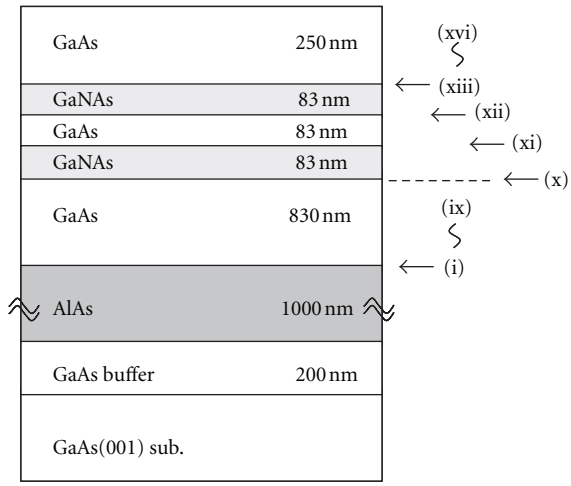

(i) Grow GaAs

(ii) Open variable leak valve

(iii) Set N_2 flow rate at 0.12 sccm

(iv) Open N shutter

(v) Close N shutter

(vi) Increase As BEP

(vii) Decrease As BEP

(viii) Turn on RF power, set at 300 W

(ix) Set N_2 flow rate at 0.02 sccm

(x) Open N shutter

(xi) Close N shutter

(xii) Open N shutter

(xiii) Close N shutter

(xiv) Turn off RF power

(xv) Set N_2 flow at 0 sccm, close VLV

(xvi) Close Ga shutter and finish the growth

Figure 10: Schematic of the sample structure with the list of growth procedures. Every step has its thickness of 83 nm except step (i) of 166 nm [32].

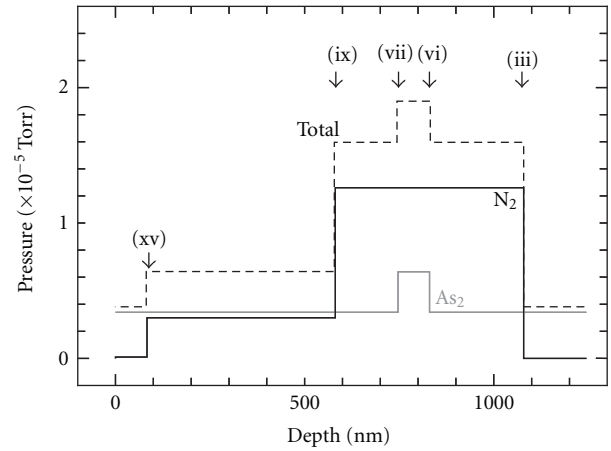

Figure 11: Partial pressures of N_2 and As_2 estimated from total background pressure [32].

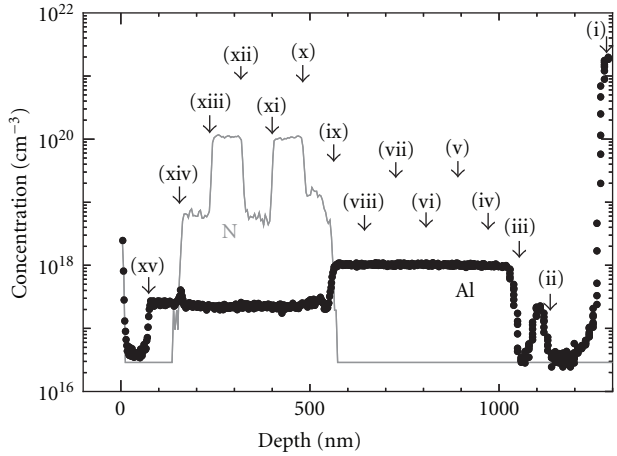

Figure 12: SIMS depth profile of N and Al for the sample shown in Figure 10 [32].

Sundgren et al. [29]. These thicknesses were chosen to resolve the effect of each operation on the concentrations of the investigated elements with SIMS measurement. The details of this procedure are as follows. Ishikawa et al. first (i) grew GaAs. During this procedure, the cell shutters of N and Al were closed and the N_2 gas flow rate was 0 sccm. They (ii) opened the variable leak valve (VLV), which was attached between the mass flow controller (MFC) and the plasma cell, and (iii) set the N_2 gas flow rate to 0.12 sccm to supply a sufficient amount of N_2 gas that would enable the succeeding plasma ignition. They (iv) opened and (v) closed the N shutter to examine these effects. To examine the effect of As flux, they increased and decreased its beam equivalent pressure (BEP) in steps (vi) and (vii), as shown in Figure 11. The As_2 BEP of 3.5×10^{-6} Torr in step (vii) is the standard growth condition for GaAs at 1.0 ML/s in their MBE system. They (viii) turned on the RF power of the plasma cell and adjusted it to 300 W where N plasma ignites in dark mode. In step (ix), the N_2 flow rate was decreased to 0.02 sccm to make the plasma transfer to bright mode. In steps (x)–(xiii), they opened and closed the shutter of the N plasma cell and repeated this twice to accurately examine its effect. In step (xiv), the RF power was turned off and then the plasma was extinguished. In step (xv), the N_2 flow rate was set to zero and VLV was closed. The shutter of the Ga cell was closed to finish growth in step (xvi).

Figure 12 shows the SIMS depth profiles of N and Al for the sample. The N concentration is preferably controlled by the applied power, flow rate, resulting plasma mode transfer, and its shutter operation. Aluminum was incorporated in spite of the closed shutter of the Al cell. When the VLV was opened in step (ii), the Al profile showed a peak. The largest concentration of $1.0 \times 10^{18}\,cm^{-3}$ was observed between steps (iii) and (viii). The concentration decreased to $2 \times 10^{17}\,cm^{-3}$ in step (ix), maintaining that amount until step

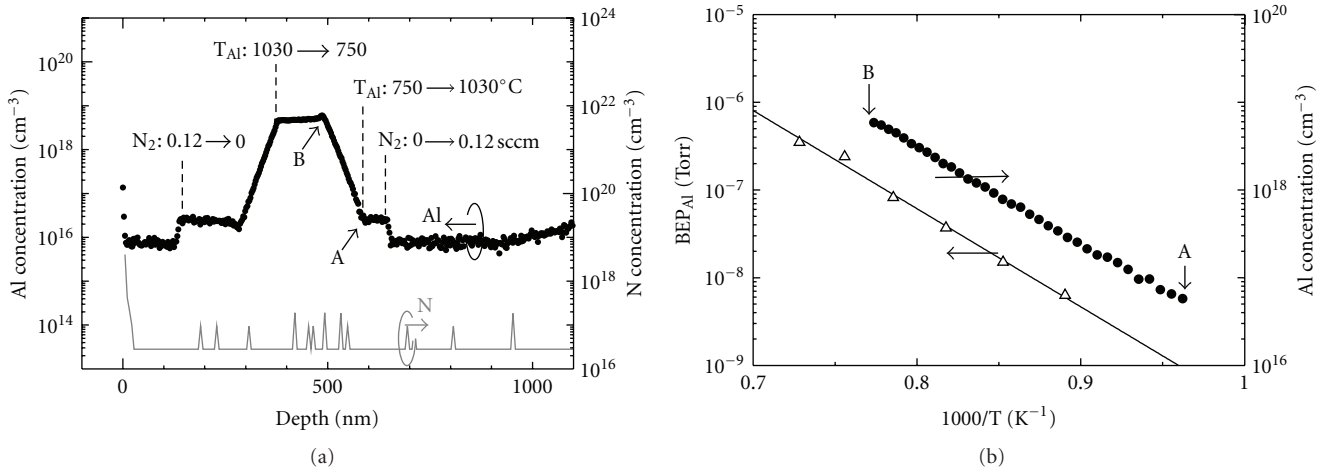

FIGURE 13: (a) SIMS depth profile of Al and N for the sample grown at various T_{Al} values as indicated. N_2 gas flowed at the indicated points. (b) Plots of Al vapor pressure and concentration of incorporated Al as functions of reciprocal temperature. The solid line indicates a linear fit on the results [33].

(xv). The concentration then dropped to 3×10^{16} cm^{-3}. The above results cannot be due to the failure of the shutter control since Al concentration was suppressed in steps (i) and (xv) where N was not introduced. These results cannot be related to the diffusion or segregation from the AlAs layer, as mentioned by Sundgren et al. [29] since the incorporation of Al was not detected in the GaAs layer in step (i) locating just above the AlAs layer. Consequently, the Al concentration solely depends on the N_2 flow rate and the vapor pressures of N_2. The plasma power, mode, shutter conditions, and As flux that varied within the parameters had no impact. A peak observed in step (ii) probably resulted from the residual N_2 gas remaining at the gas line between VLV and MFC. It was evacuated in about 1 min corresponding to the 16 nm GaAs growth, which agreed well with the peak widths. Since the variation in As BEP has no impact on the concentration of extrinsic Al, the phenomena observed are considered due to the specific characteristics of N_2 under their conventional growth conditions.

Ishikawa et al. also investigated the correlation between the vapor pressures of N and Al to ascertain the origin of the incorporated Al [33]. They carried out an experiment similar to the one above at various Al vapor pressures during growth. Figure 13(a) shows the SIMS results for the sample. They used a lower growth rate of 0.3 ML/s to efficiently detect unintentional Al flux. The N plasma was not ignited throughout growth. Initially, the temperature of the Al cell (T_{Al}) was set at the common idling temperature of 750°C, and N_2 gas was not introduced. As indicated in the figure, they introduced the N_2 gas at a flow rate of 0.12 sccm for a certain period. After that, they shut off the flow. Within this period, they increased and decreased T_{Al} to vary the vapor pressure of Al. At position A, indicated in the figure, they started to increase T_{Al} from 750°C to 1030°C at a ramp rate of 20°C/min Subsequently, T_{Al} reached 1030°C at position B. As is clearly shown in Figure 13(a), they observed Al incorporation during the period the N gas was flowing into the chamber. Moreover, the concentration depended on T_{Al}. In contrast, N was not incorporated into the sample. Figure 13(b) shows the vapor pressure and concentration of Al as functions of reciprocal temperature. Remarkably, the temperature dependences were completely identical. This result indicates that the unintentionally incorporated Al originating from the Al beam sublimated from the Al source. The Al remaining on the chamber wall, cell wall, or backside of the shutter is not likely the origin because of this temperature dependence. The Al incorporation is not followed by incorporation of N, that is, these species cannot bind to each other. The research team presumed that the introduction of N_2 gas at a high vapor pressure would modulate Al beam dispersion, resulting in an inefficient shut off of the Al flux by the shutter. This phenomenon would be similar to the case of solid-source As and Sb at a high vapor pressure. These sources show unintentional incorporation even when the mechanical shutters are closed and with concentrations at a certain proportion of the initial sublimation [34, 35].

The above results suggest that the density of incorporated Al (n_{Al}) has linear dependencies on the vapor pressures of N_2 and Al. An analytical gas-phase-scattering model reproduced these dependencies, suggesting that a large amount of N_2 gas causes the scattering of residual Al atoms with occasional collisions resulting in atoms directed toward the substrate [33]. Calculated n_{Al} agreed well with the experimental values within the errors of one order of magnitude, indicating the adequacy of the model.

2.3. Solution. As discussed above, the origin of the unintentional incorporation of Al, which generates three-dimensional growth and degrades the crystallinity of the GaInNAs active layer and LD performance, is the Al source in the MBE growth chamber. Adachi et al. made GaInNAs LDs with very low I_{th} by using a brand new Al-free MBE growth chamber [36]. They used GaInP in place of AlGaAs

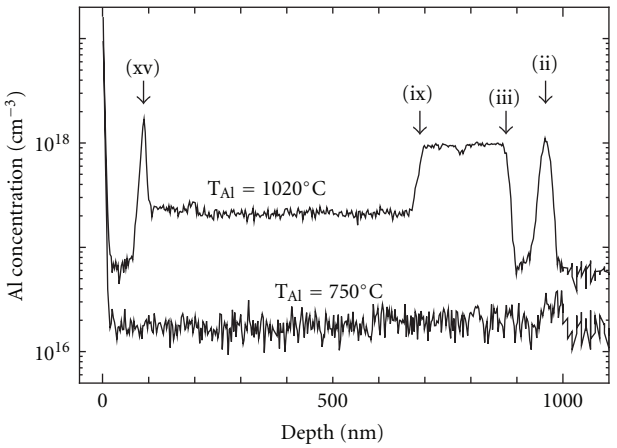

FIGURE 14: Depth profile of Al for the samples grown at the Al cell temperature (T_{Al}) of 1020°C and 750°C [32]. Those were grown with the sequences (i)–(xvi) skipping the procedures between (iv) and (vii) shown in Figure 12. The representative numbers of the steps are mentioned in Figure 10.

as the cladding layer. Although they succeeded in making excellent edge-emitting LDs, they could not make VCSELs because GaInNAs should be grown over an AlAs/GaAs DBR. Bank et al. used an MBE system with dual growth chambers [37]. One chamber was used for growing GaInNAs, and the other was for growing AlGaAs. With this MBE system, they could make VCSELs [38]; however, their MBE system is very expensive.

Figure 13 shows that Al is hardly incorporated into the epi-layer even under high vapor pressures of N_2 when T_{Al} is set at 750°C. Ishikawa et al. carried out a similar experiment to that shown in Figure 12 for two samples grown with different T_{Al} [32]. They prepared two samples grown with the same procedure of the sample shown in Figure 12, skipping steps (iv) and (vii). Figure 14 shows the Al concentration for those samples obtained by SIMS. The sample grown at T_{Al} of 1020°C exhibited a similar Al concentration profile to that in Figure 12. A peak observed at a depth around 100 nm, corresponding to step (xv), was due to the mechanical failure of the MFC. When they set the flow rate value to zero, the MFC occasionally showed spiky pressure increases, inducing the observed peak. In contrast, the sample grown at T_{Al} of 750°C showed no Al incorporation corresponding to the N gas flow rate throughout the structure. These results imply that the unintentionally incorporated Al originated from the Al beam sublimated from the Al source metal. It is difficult to determine the origin of the Al remaining on the chamber wall, cell wall, or backside of the shutter because of the dependence on cell temperature. Hence, at the common Al cell idling temperature, unintentional incorporation of Al can be efficiently suppressed even though the MBE chamber has an Al cell and epilayers containing Al have been grown inside.

The introduction of N may also enhance the concentration of other undesirable impurities such as C and O, possibly originating from the constituents of N gas or residuals in the chamber. These impurities may be harmful to the epitaxial layers, resulting in poorer devise performance. Ishikawa et al. carried out an experiment similar to that described in the previous section by focusing on impurities other than N and Al within the layer [33]. Figures 15(a) and 15(b) show SIMS results for samples grown at different T_{Al} of 1020 and 750°C, respectively. The concentrations of C, O, Al, and S are plotted in the figures against the N_2 gas flow rates of 0 and 0.12 sccm, at which the N_2 gas shows its partial pressures of 0 and 1.3×10^{-5} Torr, respectively. The growth rate was 1.0 ML/s. Sulfur stemming from epiready treatment was observed within the samples. The S concentration was 1×10^{15} cm^{-3}, which does not depend on T_{Al} and N_2 gas flow rate. In contrast, the concentrations of C, O, and Al varied with changes in the above parameters. At T_{Al} of 1020°C shown in Figure 15(a), the concentration of Al clearly increased following the introduction of N_2 gas. Furthermore, C and O also showed similar behavior. In contrast, at T_{Al} of 750°C, as shown in Figure 15(b), the dependence on N_2 gas flow rate was solely observed for O and was negligible for C and Al. Oxygen concentration showed a dependence on the N_2 gas flow rate but was much smaller, over one order of magnitude, than that shown in Figure 15(a). It was as low as 2×10^{16} cm^{-3} even with the N_2 gas flow rate of 0.12 sccm. This result indicates that a heated Al cell and Al partial pressure can enhance O incorporation into the epitaxial layer. It should be noted that they have also measured the concentration of N on the layer, not shown in Figure 15, since it was below the detection limit. These may result from the getter effect of Al, which would be effective for O, which has a strong affinity to Al, but not with inert N_2 gas.

The unintentional incorporation of Al and the related phenomena can result in deterioration of the epitaxial layer due to undesirable impurity incorporation and decreased diffusion length of atoms on the growing surface, which becomes pronounced at low temperatures. We should emphasize that the above phenomena are not dependent on the plasma working conditions possibly due to the dominant N_2 constituent. Thus, they arise during the entire plasma-assisted nitride growth by MBE. Accordingly, nitrides should be grown under conditions that prevent the previously described unintentional incorporation of Al by suppressing the Al partial pressure or efficient shielding of N_2 gas dispersion.

3. Summary

GaInNAs can be grown pseudomorphically on a GaAs substrate and is a light-emitting material with a bandgap energy that corresponds to near infrared. By combining GaInNAs with GaAs, an ideal band lineup for LD application is achieved. GaInNAs is also promising as a material for use in near-infrared VCSELs because a GaInNAs active layer can be grown on a highly reflective GaAs/AlAs DBR mirror over a GaAs substrate in a single stage of epitaxial growth. GaInNAs VCSELs are currently on the market.

GaInNAs can be grown by both OMVPE and MBE. However, LDs with a long lifetime are limited to MBE-grown devices. Therefore, from the viewpoint of industry

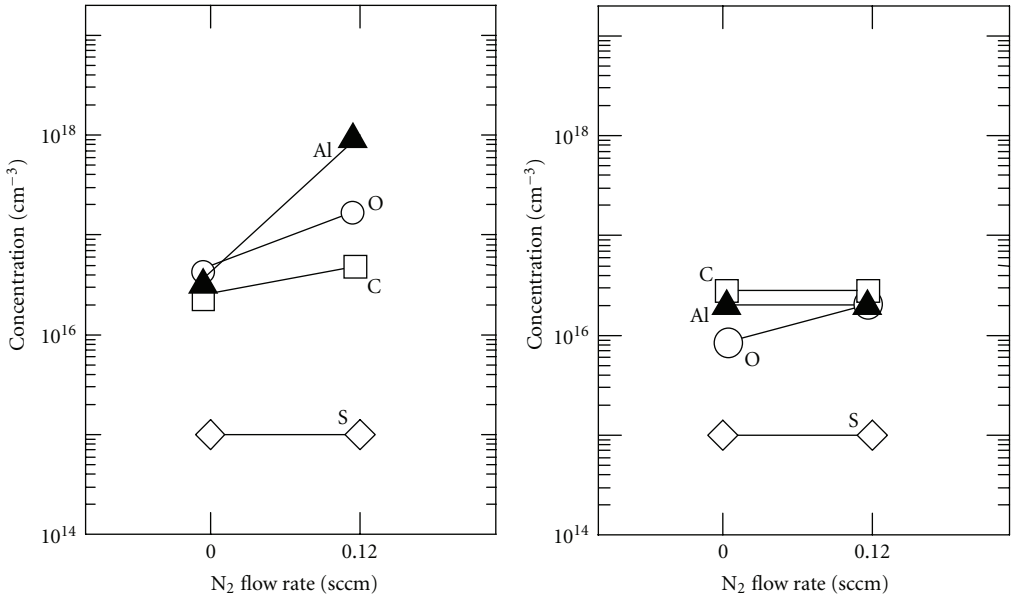

Figure 15: Concentrations of C, O, Al, and S obtained from SIMS measurement varying the N_2 gas flow rate for 0 and 0.12 sccm at different T_{Al} of (a) 1020°C and (b) 750°C [33].

use, MBE growth is important for GaInNAs. During plasma-assisted MBE growth, Al is unintentionally incorporated into the epi-layer followed by the concomitant incorporation of O and C even though the shutter of the Al cell is closed. The origin of the unintentionally incorporated Al is the Al beam sublimated from the Al source but not Al remaining on the chamber wall, cell wall, or backside of the shutter. A gas-phase-scattering model can explain these phenomena, suggesting that a large amount of N_2 gas causes the scattering of Al beam sublimated from the Al source with occasional collisions resulting in the Al atoms being directed toward the substrate. Hence, the reduction of the sublimated Al beam during the growth period can suppress the incorporation of unintentional impurities, resulting in a highly pure epitaxial layer. Thus, we can reproduce the growth of high-quality GaInNAs simply by setting the temperature of the Al cell at the common idling temperature of 750°C, even though the MBE chamber has an Al cell and epilayers containing Al have been grown inside.

The above phenomena are not dependent on the plasma working conditions, possibly due to the dominant N_2 constituent. Thus, they arise during the entire plasma-assisted nitride growth by MBE. Accordingly, nitrides should be grown under conditions that prevent the above-described unintentional incorporation of Al by suppressing the Al partial pressure or efficient shielding of N_2 gas dispersion.

References

[1] M. Kondow, K. Uomi, A. Niwa, T. Kitatani, S. Watahiki, and Y. Yazawa, "A novel material of GaInNAs for long-wavelength-range laser diodes with excellent high-temperature performance," in *Proceedings of the International Conference on Solid State Devices and Materials*, Osaka, Japan, 1995.

[2] M. Kondow, K. Uomi, A. Niwa, T. Kitatani, S. Watahiki, and Y. Yazawa, "GaInNAs: a novel material for long-wavelength-range laser diodes with excellent high-temperature performance," *Japanese Journal of Applied Physics 1*, vol. 35, no. 2, pp. 1273–1275, 1996.

[3] J. N. Baillargeon, K. Y. Cheng, G. E. Hofler, P. J. Pearch, and C. Heigh:, "Luminescence quenching and the formation of the $GaP_{1-x}N_x$ alloy in GaP with increasing nitrogen content," *Applied Physics Letters*, vol. 60, article 2540, 3 pages, 1992.

[4] O. Igarashi, "Heteroepitaxial growth of $GaP_{1-x}N_x(x \lesssim 0.09)$ on sapphire substrates," *Japanese Journal of Applied Physics*, vol. 31, article 3791, 1992.

[5] S. Miyoshi, H. Yaguchi, K. Onabe, R. Ito, and Y. Shiraki, "Metalorganic vapor phase epitaxy of $GaP_{1-x}N_x$ alloys on GaP," *Applied Physics Letters*, vol. 63, no. 25, pp. 3506–3508, 1993.

[6] M. Sato and M. Weyers, "GaAsN alloys: growth and optical properties," in *Proceedings of the 19th International Symposium on GaAs and Related Compound Semiconductors*, vol. 129 of *Institute of Physics Conference*, pp. 555–560, Bristol and Philadelphia: Institute of Physics, Karuizawa, Japan, 1992.

[7] M. Kondow, K. Uomi, K. Hosomi, and T. Mozume, "Gas-source molecular beam epitaxy of GaN_xAs_{1-x} using a N radical as the N source," *Japanese Journal of Applied Physics 2*, vol. 33, no. 8, pp. L1056–L1058, 1994.

[8] S. Sato, "Room temperature operation of InGaNAs/InGaP DH lasers grown by MOCVD," in *Proceedings of the 57th Autumn Meeting Japan Society of Applied Physics*, p. 951, Fukuoka, Japan, 1996.

[9] M. Kondow, T. Kitatani, M. C. Larson, K. Nakahara, K. Uomi, and H. Inoue, "Gas-source MBE of GaInNAs for long-wavelength laser diodes," *Journal of Crystal Growth*, vol. 188, no. 1–4, pp. 255–259, 1998.

[10] S. Sakai, Y. Ueta, and Y. Terauchi, "Band gap energy and band lineup of III-V alloy semiconductors incorporating nitrogen

and boron," *Japanese Journal of Applied Physics 1*, vol. 32, no. 10, pp. 4413–4417, 1993.

[11] J. C. Phillips, *Bonds and Bands in Semiconductors*, Academic Press, New York, NY, USA, 1973.

[12] T. Kitatanl, M. Kondow, T. Klkawa, Y. Yazawa, M. Okai, and K. Uomi, "Analysis of band offset in GaNAs/GaAs by x-ray photoelectron spectroscopy," *Japanese Journal of Applied Physics 1*, vol. 38, no. 9, pp. 5003–5006, 1999.

[13] S. A. Ding, S. R. Barman, K. Horn et al., "Valence band discontinuity at a cubic GaN/GaAs heterojunction measured by synchrotron-radiation photoemission spectroscopy," *Applied Physics Letters*, vol. 70, no. 18, pp. 2407–2409, 1997.

[14] S. Sakai and T. Abe, "Band lineup of nitride-alloy heterostructures," in *Proceedings of the 41st Spring Meeting of the Japan Society of Applied Physics*, p. 186, Tokyo, Japan, 1994.

[15] M. Kondow, S. Fujisaki, S. Shirakata, T. Ikari, and T. Kitatani, "Electron effective mass of $Ga_{0.7}In_{0.3}N_xAs_{1-x}$," in *Proceedings of the 30th International Symposium on Compound Semiconductors*, MB 3.8, San Diego, Calif, USA, 2003.

[16] C. Skierbiszewski, P. Perlin, P. Wisniewski et al., "Effect of nitrogen-induced modification of the conduction band structure on electron transport in GaAsN alloys," *Physica Status Solidi B*, vol. 216, no. 1, pp. 135–139, 1999.

[17] Z. Pan, L. H. Li, Y. W. Lin, B. Q. Sun, D. S. Jiang, and W. K. Ge, "Conduction band offset and electron effective mass in GaInNAs/GaAs quantum-well structures with low nitrogen concentration," *Applied Physics Letters*, vol. 78, no. 15, pp. 2217–2219, 2001.

[18] M. Hetterich, M. D. Dawson, A. Y. Egorov, D. Bernklau, and H. Riechert, "Electronic states and band alignment in GalnNAs/GaAs quantum-well structures with low nitrogen content," *Applied Physics Letters*, vol. 76, no. 8, pp. 1030–1032, 2000.

[19] M. C. Larson, M. Kondow, T. Kitatani et al., "GaInNAs-GaAs long-wavelength vertical-cavity surface-emitting laser diodes," *IEEE Photonics Technology Letters*, vol. 10, no. 2, pp. 188–190, 1998.

[20] M. Kondow, T. Kitatani, K. Nakahara, and T. Tanaka, "A 1.3-μm GaInNAs laser diode with a lifetime of over 1000 hours," *Japanese Journal of Applied Physics 2*, vol. 38, no. 12, pp. L1355–L1356, 1999.

[21] J. Jewell, L. Graham, M. Crom et al., "Commercial GaInNAs VCSELs grown by MBE," *Physica Status Solidi C*, vol. 5, no. 9, pp. 2951–2956, 2008.

[22] I. Buyanova and W. Chen, *Physics and Applications of Dilute Nitrides*, Taylor & Francis, New York, NY, USA, 2004.

[23] N. Tansu, J. Y. Yeh, and L. J. Mawst, "Low-threshold 1317-nm InGaAsN quantum-well lasers with GaAsN barriers," *Applied Physics Letters*, vol. 83, no. 13, pp. 2512–2514, 2003.

[24] S. M. Wang, Y. Q. Wei, X. D. Wang, Q. X. Zhao, M. Sadeghi, and A. Larsson, "Very low threshold current density 1.3 μm GaInNAs single-quantum well lasers grown by molecular beam epitaxy," *Journal of Crystal Growth*, vol. 278, no. 1–4, pp. 734–738, 2005.

[25] R. Fehse, S. Jin, S. J. Sweeney et al., "Evidence for large monomolecular recombination contribution to threshold current in 1.3 μm GaInNAs semiconductor lasers," *Electronics Letters*, vol. 37, no. 25, pp. 1518–1520, 2001.

[26] S. Nakatsuka, M. Kondow, M. Aoki, M. Kudo, T. Kitatani, and S. Tsuji, "Amplified spontaneous emission measurement of GaInNAs laser wafers with and without rapid thermal annealing," *Japanese Journal of Applied Physics 2*, vol. 42, no. 8, pp. L1012–L1014, 2003.

[27] T. Takeuchi, Y. L. Chang, M. Leary et al., "Al contamination in InGaAsN quantum wells grown by metalorganic chemical vapor deposition and 1.3 μm InGaAsN vertical cavity surface emitting lasers," *Japanese Journal of Applied Physics 1*, vol. 43, no. 4, pp. 1260–1263, 2004.

[28] T. Takahashi, M. Kaminishi, N. Jikutani, A. Itoh, and S. Sato, "Improvement of the optical property of 1 step MOCVD grown GaInNAs/GaAs MQW on AlGaAs cladding layer," in *Procedings of the 64th Autumn Meeting of the Japan Society of Applied Physics*, 1p-K-18, Fukuoka, Japan, 2003.

[29] P. Sundgren, C. Asplund, K. Baskar, and M. Hammar, "Morphological instability of GaInNAs quantum wells on Al-containing layers grown by metalorganic vapor-phase epitaxy," *Applied Physics Letters*, vol. 82, no. 15, pp. 2431–2433, 2003.

[30] M. Kondow, M. Kudo, S. Tanaka, S. Fujisaki, and K. Nakahara, "Residual impurities in MBE-grown GaInNAs laser diodes," in *Proceedings of the 13th International Conference on Molecular Beam Epitaxy*, TuC2.5, Edinburgh, UK, 2004.

[31] T. Kitatani, M. Kondow, and T. Tanaka, "Molecular beam epitaxy of GaInNAs by using solid source arsenic," *Journal of Crystal Growth*, vol. 227-228, pp. 521–526, 2001.

[32] F. Ishikawa, S. D. Wu, M. Kato, M. Uchiyama, K. Higashi, and M. Kondow, "Unintentional aluminum incorporation related to the introduction of nitrogen gas during the plasma-assisted molecular beam epitaxy," *Journal of Crystal Growth*, vol. 311, no. 7, pp. 1646–1649, 2009.

[33] F. Ishikawa, S. Wu, M. Kato, M. Uchiyama, K. Higashi, and M. Kondow, "Unintentional source incorporation in plasma-assisted molecular beam epitaxy," *Japanese Journal of Applied Physics*, vol. 48, no. 12, Article ID 125501, 2009.

[34] J. Schmitz, J. Wagner, M. Maier, H. Obloh, P. Koidl, and J. D. Ralston, "Unintentional As incorporation in molecular beam epitaxially grown InAs/AlSb/GaSb heterostructures," *Journal of Electronic Materials*, vol. 23, no. 11, pp. 1203–1207, 1994.

[35] C. E. C. Wood, T. M. Kerr, T. D. McLean et al., "State-of-the-art AlGaAs alloys by antimony doping," *Journal of Applied Physics*, vol. 60, no. 4, pp. 1300–1305, 1986.

[36] K. Adachi, K. Nakahara, J. Kasai et al., "Low-threshold GaInNAs single-quantum-well lasers with emission wavelength over 1.3μm," *Electronics Letters*, vol. 42, no. 23, pp. 1354–1355, 2006.

[37] S. R. Bank, H. Bae, L. L. Goddard et al., "Recent progress on 1.55-μm dilute-nitride lasers," *IEEE Journal of Quantum Electronics*, vol. 43, no. 9, pp. 773–785, 2007.

[38] M. A. Wistey, S. R. Bank, H. B. Yuen, L. L. Goddard, and J. S. Harris, "GaInNAs(Sb) vertical-cavity surface-emitting lasers at 1.460 μm," *Journal of Vacuum Science and Technology B*, vol. 22, no. 3, pp. 1562–1564, 2004.

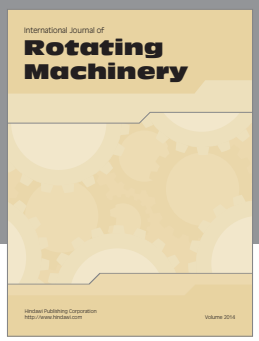

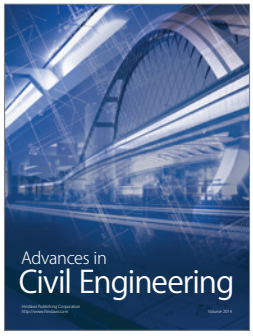

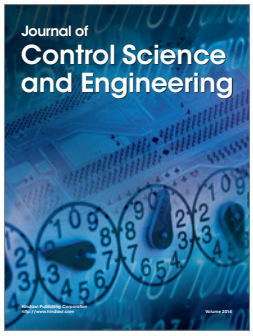

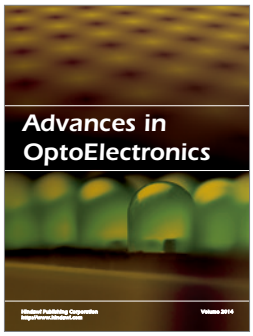

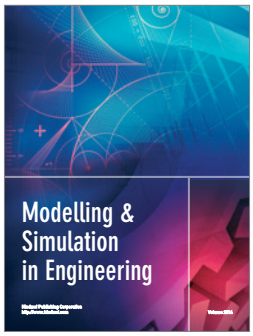

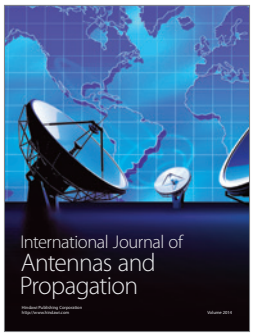

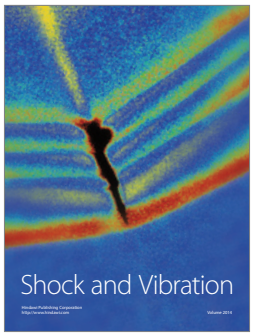

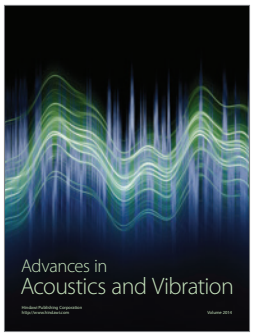

Hindawi

Submit your manuscripts at
http://www.hindawi.com